J. Fluid Mech. (1969), *vol.* 35, *part* 4, *pp.* 721–735
Printed in Great Britain

The fluid mechanics of the aortic valve

By B. J. BELLHOUSE AND L. TALBOT†
Department of Engineering Science, Oxford University

(Received 10 June 1968)

The closure mechanism of the human aortic valve is investigated experimentally with a rigid-walled model placed in a pulsatile water-tunnel. It is shown that the valve is controlled by a fluid feed-back system incorporating a stagnation point at the downstream end of each sinus and a trapped vortex within it, and that threequarters of the valve's closure is accomplished during forward flow, requiring only very little reversed flow to seal it. The experiments are complemented by solutions of the inviscid-flow equations, based on a Hill spherical vortex model.

Introduction

The heart consists of two pumps, the right side supplying the lungs, the left pumping oxygenated blood through the body. The pumps consist of a collecting chamber (atrium) a muscular-pumping chamber (ventricle) and an outlet pipe. There are non-return valves between the ventricle and the atrium and between the outlet pipe and the ventricle. The valves, particularly of the left side of the heart, are prone to disease and may have to be replaced, but their mechanical substitutes usually damage the red cells in the blood. The outlet pipe to the left ventricle is called the aorta and the valve between the left ventricle and the aorta is known as the aortic valve. It consists of three non-muscular flaps (cusps) only 0·1 mm thick which open and close once a second for about 70 years and support a pressure difference of 100 mm of mercury when closed.

A photograph of a human aortic vale is shown in figure 1, plate 1. The ventricle (V) is at the bottom and the smooth wall of the aorta (A) at the top. The valve has been cut open, so the extreme left- and right-hand sides of the photograph correspond to each other. The cusps (C) and sinuses (S) are clearly visible and so are the sinus ridges (R) which are a marked feature. The position of a coronary ostium (O) is close to the sinus ridge, but within the sinus. The significance of this, and other features of the aortic root, are discussed more fully in another paper (Bellhouse & Reid 1968).

The mechanism of the aortic valve has prompted speculation and experiment since the Renaissance. The majority of these theories have visualized the blood leaving the left ventricle as a jet, but our own measurements show that the velocity profile, within one diameter of the valve, is flat. Other theories depend on elastic recoil of the aortic wall to close the valve. One of the earliest theories, and certainly one of the best, was advanced by Leonardo da Vinci (1513), who

† Permanent address: University of California, Berkeley.

realized that there were always three marked dilatations of the aorta, called sinuses, one corresponding to each cusp of the valve. He correctly predicted that vortices would be formed in the sinuses and that they would feature in the control mechanism of the valve. Leonardo was ignorant of the circulation of the blood and incorrectly ascribed other functions to the vortices, which he supposed persisted for many heart-beats and dissipated energy to generate heat. The first anatomical account of the aortic sinuses was published by Valsalva (1740), who was struck by the uniform presence of sinuses in a variety of birds and mammals and concluded that they must serve a common purpose in all these creatures. He suggested that their main function was to dissipate the violence of systolic contraction by allowing blood to enter the sinuses during systole, which is the period when the ventricle is ejecting blood. Since about 75 cm^3 is ejected each beat, the sinuses are too small to perform this function.

The constancy of the proportions of the aortic valve in mammals suggests that all have the same mechanism, so we built a model of the valve with an aortic diameter of 2·5 cm, about the size of a human aorta. The valve was made of Perspex, except for the cusps which were 0·1 mm thick nylon net impregnated with silastic. The cusps were relaxed in the open position so that any elastic recoil they might have would work against closure. Since the sinuses were made of Perspex, they were inelastic; when flexible sinuses were fitted the performance of the valve was unaltered. One anatomical feature which is most marked is a ridge at the downstream end of the sinus, marked R in figure 1, and this was copied in the model.

The model was placed in a pulsatile water-tunnel, which permitted independently adjustable steady and sinusoidal flow-components. Care was taken to settle, straighten and contract the flow in order to present the valve with a laminar, uniform stream. The pulse could be adjusted to resemble the physiological systolic flow-pulse, although the diastolic phases (during which the ventricle fills) did not match. However, the diastolic phase is of no interest in the study of the fluid dynamics of the aortic valve, since the valve is closed throughout.

The results of some simple experiments are described by Bellhouse & Bellhouse (1968).

In steady or pulsatile flow, intense vortices could be seen to form in the sinuses of Valsalva. In pulsatile flow they persisted throughout systole and the valve could be seen to close slowly and evenly, performing much of its closure movement during forward flow. Measurement of mean forward flow by timing a given discharge from the water-tunnel, and measurement of maximum reversed flow, with dye, together with a measurement of pulse rate, proved to be a simple way of assessing the efficiency of the valve. This is defined as the net forward flow per pulse multiplied by 100 and divided by the peak forward flow per pulse. The valve was more than 98 % efficient. However, for an identical set of cusps placed in a tube without sinuses, no stagnation point and no vortex could form and the valve was only 75 % efficient and was closed by reversed flow suddenly and unevenly. The importance of the sinuses was clearly demonstrated, but the exact functions of the vortex and the stagnation point in each sinus remained obscure. In pulsatile flow, the cusps remained fully open for over half of systole, so this phase was not dissimilar to steady flow, which is taken as our starting point.

Steady flow

With a steady velocity of 62·3 cm/sec in the aorta, the cusps were positioned as in figure 2 with a dividing streamline meeting the sinus ridge at S, opposite the centre of the cusp tip. With the use of dye, the vortex pattern, generated by a complex inflow–outflow system at the downstream end of the sinuses, could be observed. Each vortex occupied the entire sinus, but the core was located near

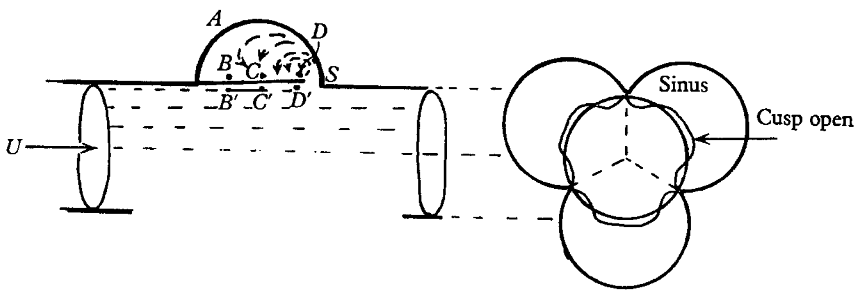

FIGURE 2. Streamlines for steady flow.

the cusp tip. This observation was confirmed by velocity measurements using a heated-film anemometer, with free-stream values attained within the sinus near the cusp tip, and lower velocities deeper in the sinus. The pressure on the sinus ridge was measured to be 0·935 ($\frac{1}{2}\rho U^2$) above free stream static pressure (where ρ is the fluid density, and U the aortic velocity) which showed that its pressure was close to the free-stream stagnation value. The pressure reduced rapidly along the curved sinus wall, with values at A, B, C and D in figure 2 of (0·353, 0·227, 0·176, 0·176)$\frac{1}{2}\rho U^2$. The pressures at B', C', D' matched the pressures at B, C, D respectively and there was no radial variation of pressure in the aorta. The aortic pressures implied that the cusps bulged into the sinuses by about 1 mm on average, and this was confirmed by observation, for the centre of the cusp appeared to be about 2 mm into the sinus, with the corners projecting slightly into the aorta.

When a 2 mm sleeve was fixed into the aorta, level with S, to reduce the diameter of the aorta downstream of the sinuses, the cusps were observed to relign, again about 1 mm outside the line of the new sinus ridge. In neither case did the cusps flutter, which implied a stable fluid dynamic control system. Equilibrium was established with a balance of flow in and out of the sinuses, with the centre of the sinus ridge (S), maintained at free-stream stagnation pressure.

The vortex is generated by flow in and out of the sinus, which is maximal in the equilibrium position of the cusp. If the cusp were deflected into the sinus, the vortex strength would be reduced and the sinus pressure would approach stagnation values which would restore the cusp to its equilibrium position. If the cusp were deflected away from the sinus, the stagnation point would be replaced by a reattachment point further downstream, and sinus pressure would approach the pressure at the cusp tips, which will be below the free-stream value because of the narrowing of the orifice, and the cusps will again return to their equilibrium position.

Steady flow analysis of the behaviour of a vortex in a hemispherical cavity

Our model of the sinus vortex is one half of a Hill spherical vortex as, for example, described in Milne-Thomson (1960, pp. 553–4). We imagine that the aortic valve in its fully open position forms a plane surface bounding the major portion of the sinus and that both the aorta and sinus are of radius a. The cusp is of length $\frac{3}{2}a$ along its major dimension and the flow in the aorta is assumed uniform and of velocity U (figure 3).

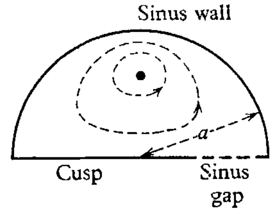

FIGURE 3. Sinus vortex model.

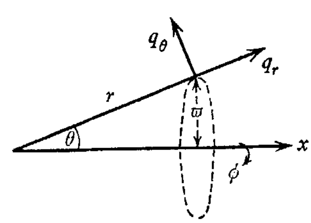

FIGURE 4. Spherical polar co-ordinates.

The stream function, ψ, for the Hill vortex in steady flow is given by

$$\psi = -\tfrac{1}{10}A\,(a^2-r^2)\,r^2\sin^2\theta \tag{1}$$

and the associated velocities are

$$\left.\begin{aligned} q_r &= -\frac{1}{r^2\sin\theta}\frac{\partial\psi}{\partial\theta} = \frac{A}{5}\,(a^2-r^2)\cos\theta,\\ q_\theta &= \frac{1}{r\sin\theta}\frac{\partial\psi}{\partial r} = -\frac{A}{5}\,(a^2-2r^2)\sin\theta \end{aligned}\right\} \tag{2}$$

in the spherical co-ordinate system shown in figure 4.

The vorticity, curl $\mathbf{q}$, has only one component, ζ, in the ϕ-direction; that is, the vorticity is everywhere perpendicular to meridianal planes passing through the axis of symmetry, so that vortex lines are circles of radius $\varpi = r\sin\theta$ and the magnitude of the vorticity is

$$\zeta = Ar\sin\theta = \frac{1}{r}\frac{\partial}{\partial r}(rq_\theta) - \frac{1}{r}\frac{\partial q_r}{\partial\theta}. \tag{3}$$

The stagnation points of the Hill vortex occur at $r = a$, $\theta = 0, \pi$ and there is also a ring of stagnation points on the circle $r = a/\surd 2$, $\theta = \frac{1}{2}\pi$, which corresponds to the core of the vortex. In the full Hill spherical vortex, all vortex lines are closed circles, but in our hemispherical model all vortex lines, including the core, terminate at two symmetrical points on the surface of the cusps, except for the region of the sinus gap (see figure 3), where a complicated inflow–outflow pattern exists which is not accounted for in our model. This point is discussed in more detail below. Although viscous effects undoubtedly play some role in the vortex motion, we expect that the pressure distribution around the vortex, which is of chief concern to us, will be determined mainly by the motion of an essentially inviscid vortex core, in the manner envisaged by Batchelor (1956) and confirmed by Burggraf (1966). Also, the outflow from the corners of the sinuses undoubtedly convects vorticity downstream into the aorta, in a manner akin to that of the trailing vortices behind a finite wing and this effect is likewise not included in our model.

The vorticity at the vortex core is, from (3),

$$\zeta_0 = Aa/\surd 2. \tag{4}$$

When viscous and body forces are absent, as in the case of the Hill vortex, the total head $H = (p/\rho) + \frac{1}{2}q^2 (q^2 = q_r^2 + q_\theta^2$ and p and ρ are pressure and density respectively) is given by the equation of motion,

$$\mathbf{q} \wedge \boldsymbol{\zeta} = \nabla H + (\partial \mathbf{q}/\partial t) \tag{5}$$

and from this we find that for steady flow, with $\partial \mathbf{q}/\partial t = 0$,

$$\left.\begin{aligned} \partial H/\partial r &= q_\theta \zeta, \\ \partial H/\partial \theta &= -rq_r\zeta, \end{aligned}\right\} \tag{6}$$

which, on substitution of (2) and (3) and after integration yields

$$H = -\tfrac{1}{10}A^2(a^2r^2 - r^4)\sin^2\theta + C. \tag{7}$$

In (7) the constant of integration C is evaluated by requiring that at the stagnation points $r = a$, $\theta = 0, \pi$ the pressure be the stagnation pressure at the sinus ridge, p_0. Thus, at $r = a$, $\theta = 0, \pi$, $H = C = p_0/\rho$, and the total head is

$$H = \frac{p}{\rho} + \tfrac{1}{2}q^2 = \frac{p_0}{\rho} - \frac{A^2}{10}(a^2r^2 - r^4)\sin^2\theta. \tag{8}$$

It is natural to enquire whether diffusive processes are adequate for transporting vorticity from the boundary layer on the aortic side of the cusp, across the sinus gap into the sinus. From the theory of unsteady laminar boundary layers (and, it should be noted, the flow in a healthy aorta is laminar) we know that the time t_D for diffusion of vorticity over a distance a is of order of magnitude

$$t_D \sim a^2/\nu \tag{9}$$

where ν is the kinematic viscosity. If $a = 1{\cdot}0$ cm and $\nu = 3{\cdot}5 \times 10^{-2}$ cm^2/sec, values typical of the human system, then $t_D \sim 28$ sec. In pulsatile flow, the vortex must be established in much less than a second, so the vorticity contained in the sinus can only be accounted for by convective transport, that is, by a combined inflow–outflow process which establishes circulatory motion within the sinus and this is what is observed in the experiments. The time necessary to generate the sinus vortex by convective processes, t_c, is roughly the time necessary for a fluid particle to make one circuit of the vortex, of radius a at free-stream velocity U, so

$$t_c \sim \frac{(2+\pi)a}{U}. \tag{10}$$

Taking $a = 1{\cdot}0$ cm, $U = 100$ cm/sec, at peak systole, $t_c \sim 0{\cdot}05$ sec, which is the correct order of magnitude.

If we assume that the vortex is generated by convective processes and can be dissipated only by viscosity during forward flow then we require that $t_c \ll 1/f$ and $t_D \gg 1/f$ since $1/f$ is the duration of one heart beat. The first condition gives an upper bound of Strouhal number (fa/U) and the ratio t_D/t_C a lower bound of Reynolds number (Ua/ν). Bellhouse & Reid (1968) computed the values of Reynolds and Strouhal numbers for the elephant, the mouse and man:

	Ua/ν	fa/U
Mouse	186	0·0089
Man	4,458	0·0434
Elephant	11,794	0·0756

If we take $t_c \leqslant 0{\cdot}1/f$ and $t_D \geqslant 10/f$, we obtain an upper bound of Strouhal number of 0·1 and a lower bound of Reynolds number of 100.

Since convective effects are responsible for the formation of the sinus vortex, we may estimate the factor A by supposing that the vortex strength, and in particular the vorticity at its core, is proportional to the angular velocity of the inflow to the sinus and put

$$\zeta_0 = \alpha U/a, \tag{11}$$

where α is a constant. Since $\zeta_0 = Aa/\surd 2$, we have

$$A = \frac{\surd 2\, \alpha U}{a^2}. \tag{12}$$

From equations (2), (8) and (12) and denoting the sinus and aortic pressures by p_s and p_∞ respectively, we obtain

$$\frac{p_s - p_\infty}{\frac{1}{2}\rho U^2} = 1 - 0{\cdot}08\alpha^2\left\{1 - 2\left(\frac{r}{a}\right)^2 + \left(\frac{r}{a}\right)^4 + \sin^2\theta\left(3\left(\frac{r}{a}\right)^2 - 2\left(\frac{r}{a}\right)^4\right)\right\}. \tag{13}$$

Writing the velocity as

$$q \equiv (q_r^2 + q_\theta^2)^{\frac{1}{2}} \tag{14}$$

we obtain

$$q^2 = 0{\cdot}08\alpha^2 U^2\left\{1 - 2\left(\frac{r}{a}\right)^2 + \left(\frac{r}{a}\right)^4 + \sin^2\theta\left(3\left(\frac{r}{a}\right)^4 - 2\left(\frac{r}{a}\right)^2\right)\right\}. \tag{15}$$

Denoting the average sinus pressure on the cusps, obtained by integrating p_s over the cusp surface, by $\overline{p}_s$ we have

$$\frac{\overline{p}_s - p_\infty}{\frac{1}{2}\rho U^2} = 1 - 0{\cdot}0672\alpha^2. \tag{16}$$

Matching the measured pressure coefficient at C in figure 2 with (13) and $r = 0$ we find that $\alpha = 3{\cdot}21$ and the pressure coefficient in (16) is $0{\cdot}308$.

The peak velocity is attained at $r = 0$ and at $r = a$, $\theta = \frac{1}{2}\pi$ from (15) and is found to be $0{\cdot}91U$. This is in agreement with experiment, although the peak values in velocity were attained more towards the sinus ridge. A better solution than the Hill vortex would allow for the displacement of the vortex core towards the sinus ridge, but it would add considerably to the complexity of the problem.

Pulsatile flow

The model valve was perfused with a pulsatile flow and the aortic velocity measured with a heated-element gauge (briefly described by Bellhouse & Bellhouse (1968)). The probe's output, which was proportional to instantaneous

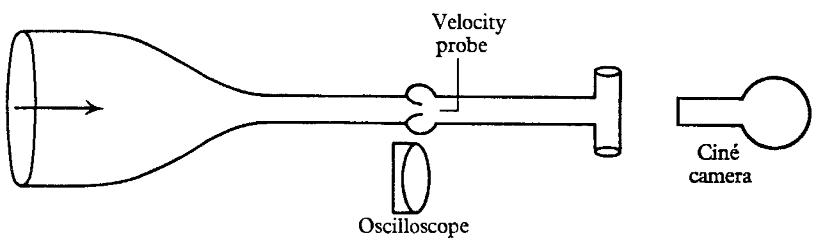

FIGURE 5. Experiment to measure simultaneously cusp position and aortic velocity.

velocity, was displayed on an oscilloscope placed level with the valve (figure 5). Using a viewer placed downstream from the valve, the cusps and oscilloscope trace were filmed simultaneously as the valve opened and closed. Analysis of the ciné film frame by frame produced the aortic velocity and valve-opening areas as functions of time, shown in figure 6. Unfortunately differential pressure gauges, suitable for use in water, and with adequate sensitivity, do not appear to be available commercially, thus reliable differential pressures were not obtained. Single-point pressure measurement was simple, using a piezo-electric gauge, but with peak-to-peak pressure variations of 200 mm of mercury, the expected differences across the cusps of about 1 mm of mercury could not be detected either by one gauge in two successive positions, or by backing off two gauges one against the other.

The model valve was filmed with two pulsatile flows, one with no flow reversal, the other with reversal sufficient to fully close the valve. The former showed that at zero velocity the cusps had swept threequarters shut, and it was confirmed visually with dye studies, that at no position in the aorta did the flow reverse. Figure 6 refers to the second pulsatile flow, with full closure of the valve after a small amount of reversed flow.

One feature of the aortic flow is that the velocity profile is flat at all phases of the cycle. This is true even at the aortic cross-section level with the sinus ridge, as can be seen in figure 7, where velocity measurements at various radial positions are shown.

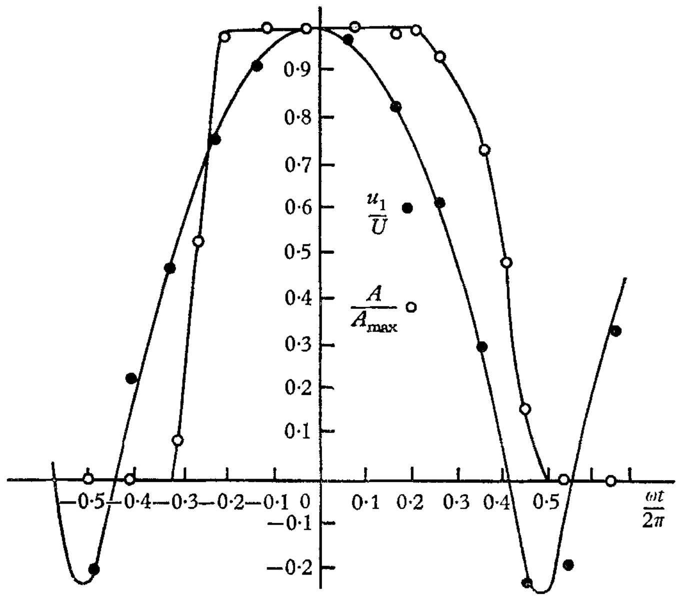

FIGURE 6. Measurements of aortic velocity and valve opening area as a function of time.

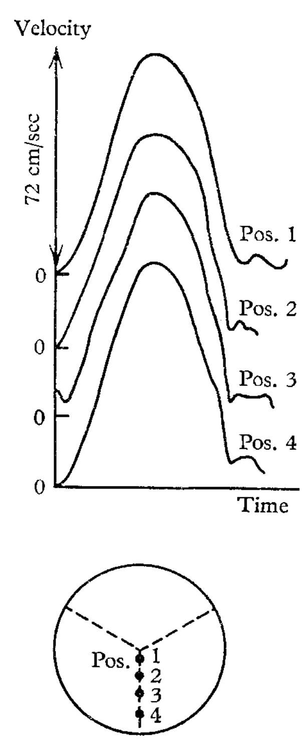

FIGURE 7. Velocity measurements level with sinus ridge.

Photographs of successive frames of a ciné film of one cycle of the valve, viewed from the aorta with forward flow approaching the camera, are shown in figure 8, plate 2. The time interval between the frames is 1/24th second, since the ciné filming was carried out at sound speed. One important feature is that the cusps are fully open by the fourth frame and are just starting to close on the eighth. There is no sign of cusp movement from the fourth to the seventh and closure is even and gradual.

These experiments enable us to construct a simple physical description of the flow patterns and pressures in the aortic root. The cycle is conveniently divided into four phases: (i) opening phase, when the cusps first bulge forward and then rapidly move to their fully open position offering no resistance to forward flow. The cusps move from shut to open positions in about 15 % of the systolic time;

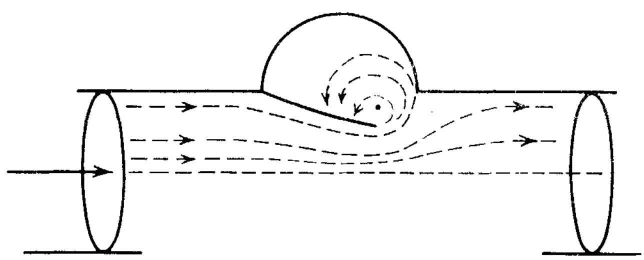

FIGURE 9. Streamlines during valve closure.

(ii) the quasi-steady phase, when the cusps make no movement and remain fully open. Although there is a variation in aortic velocity with time, at the middle of the quasi-steady phase $\partial U/\partial t$ vanishes and $\frac{1}{2}\rho U^2$ reaches its maximum, where U is the aortic velocity and t time. This phase, which occupies about 55 % of systole, is regarded as identical to the steady flow described above, except that the sinus ridge pressure will vary slowly with time; (iii) the aortic deceleration phase, when the ventricle relaxes, occupies the last 30 % of systole. An adverse pressure gradient will be established in the aorta which will cause a pressure drop across the cusps. As the cusps begin to close, fluid will be displaced and the cusp–sinus cavity enlarged. The additional flow into the sinus will continue to come from upstream and the flow pattern established in the quasi-steady phase, will persist (figure 9). This description is confirmed by the velocity traverse level with the sinus ridge, in figure 7. This mechanism spreads the streamlines downstream from the cusp tips and exploits the axial pressure gradient in order to three-quarters close the valve before forward flow ceases; (iv) the reversed flow phase, in which the cusps offer a large resistance to the reversed flow and are sealed.

Model of pulsatile flow through the valve

We assume that the flow through the valve is inviscid and the velocity varies negligibly across planes perpendicular to the axis, and that the cusps bound a cone-shaped moving surface, as in figure 10. We apply continuity and momentum equations to the control surface bounded by the cusps and the planes at the cusp tips and roots. These equations, together with an unsteady Bernoulli equation applied along the axis, which is always a streamline, enable us to calculate the pressure and velocity at the cusp tip and the average pressure difference across the cusps. We shall then relate this pressure difference to that associated with the sinus vortex.

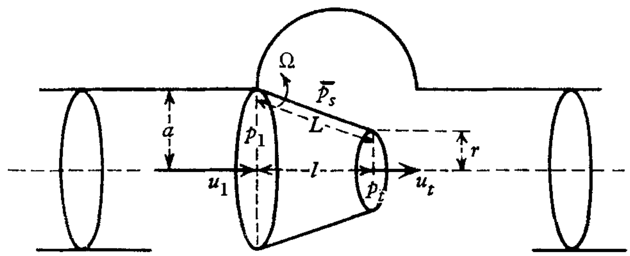

FIGURE 10. Model of pulsatile flow through the valve.

In figure 10, the cusps are of fixed length L, the angular velocity of the cusps is Ω, the aortic radius is a and the radius of the circle formed by the cusp tips is r. The pressure and velocity at the plane of the aortic ring are p_1 and u_1 respectively and at the plane of the cusp tip they are p_t and u_t. At a cross-section located at a distance x along a cusp they are p and u respectively.

Conservation of mass within the control surface S gives $\int_S \rho(\mathbf{q}\,.d\mathbf{S}) = 0$ where $\mathbf{q}$ is the fluid velocity vector. This reduces to

$$\pi a^2 u_1 - \pi r^2 u_t = \frac{dV}{dt}, \tag{17}$$

where V is the volume contained by S.

Conservation of momentum gives

$$\begin{aligned}\frac{\partial}{\partial t}\int_V \rho u \,\mathrm{d}V + \int_S \rho u(\mathbf{q}\,.d\mathbf{S}) &= \text{axial force}\\ &= \pi a^2[p_1 - \bar{p}_A + \lambda^2(\bar{p}_A - p_t)],\end{aligned} \tag{18}$$

where $\bar{p}_A$ is the average pressure on the aortic-side of the cusps and $\lambda \equiv r/a$. Equation (17) reduces to

$$u_t = \frac{u_1}{\lambda^2} - \frac{\Omega a}{3\lambda^2}\left(\frac{L}{a}\right)^2(1+2\lambda). \tag{19}$$

But (19) is valid at any cross-section within the control surface if u_t is replaced by $u(x,t)$, L by x and λ by y/a, where y is the radius of the cross-section. Thus

$$u(x,t) = \frac{a^2}{y^2}u_1 - \frac{a\Omega x^2}{3y^2}\left(1+\frac{2y}{a}\right). \tag{20}$$

By symmetry, the pipe axis is always a streamline, so the unsteady Bernoull equation can be written as

$$\int_o^l \frac{\partial u}{\partial t}\,dl + \tfrac{1}{2}[u^2]_o^l = -\frac{1}{\rho}(p_t - p_1), \tag{21}$$

where $l^2 = L^2-(a-r)^2$ from figure 10. Substituting (20) in (18) and (21), and after integration, we obtain

$$\frac{p_1-\bar{p}_A+\lambda^2(\bar{p}_A-p_t)}{\rho a} = A\frac{du_1}{dt}+Ba\frac{d\Omega}{dt}+C\frac{u_1^2}{a}+Da\Omega^2+E\Omega u_1 \quad (22)$$

and

$$\frac{p_1-p_t}{\rho a} = A_1\frac{du_1}{dt}+B_1a\frac{d\Omega}{dt}+C_1\frac{u_1^2}{a}+D_1a\Omega^2+E_1\Omega u_1, \quad (23)$$

where $A, B, \ldots, A_1, B_1, \ldots$ are functions of λ and L/a and are given in table 1.

$\lambda \equiv r/a$	A	B	C	D	E
1·0	1·500	−1·125	0	2·531	−2·250
0·9	1·497	−1·067	0·235	2·846	−2·756
0·8	1·483	−1·001	0·563	3·240	−3·485
0·7	1·470	−0·937	1·041	3·915	−4·512
0·6	1·446	−0·868	1·778	4·319	−6·051
0·5	1·414	−0·795	3·000	5·859	−8·522
λ	A_1	B_1	C_1	D_1	E_1
1·0	1·500	−1·125	0	2·531	−2·250
0·9	1·663	−1·247	0·262	3·358	−3·198
0·8	1·854	−1·390	0·722	4·645	−4·764
0·7	2·101	−1·576	1·585	6·755	−7·509
0·6	2·410	−1·807	3·362	10·513	−12·743
0·5	2·828	−2·121	7·500	18·000	−24·000

TABLE 1. Functions of λ for $L/a = 1{\cdot}5$ in (22) and (23).

With (19), (22), and (23) we can compute the pressure differences $\bar{p}_A-p_1$ and p_t-p_1 and the velocity at the cusp tip, u_t, during the deceleration phase in terms of the observed time-dependent velocity through the valve $u_1(t)$, and the observed rate of closure of the valve (from which $\Omega(t)$ can be calculated). Using the data of figure 6 with $U = 71{\cdot}2$ cm/sec, $f = 2{\cdot}28$ c/s and $a = 1{\cdot}27$ cm, we obtain the results shown in figures 11, 12, 13. In figure 11 the curve marked A is the calculated pressure difference p_t-p_1. The significance of curve B will be discussed later. These pressure differences are very small when compared with a rise and fall of static pressure of about 200 mm of mercury, and explain the inadequate performance of cusps which are too stiff. If a valve is prevented from opening fully, the vortices cannot form, and the control mechanism would be lost. Closure would be sudden and uneven, under reversed flow alone. Figure 12 shows the velocity at the cusp tip to be relatively constant during closure. Thus if the streamlines did not spread downstream of the cusp tip as in figure 9, the resultant jet would cause the sinus and cusp tip pressures $\bar{p}_s$ and p_t to be approximately equal during closure, with substantial loss of pressure difference across the cusps. The flow into the cusp-sinus cavity, calculated from the rate of displacement of fluid by the cusps, is substantial at all stages of closure (figure 13), so once the valve has begun to close, the flow pattern established in the early stages of systole will persist until foward flow ceases.

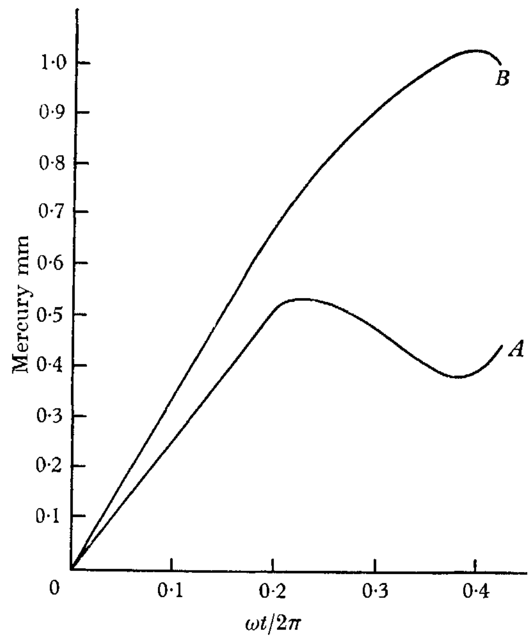

FIGURE 11. Calculated average pressure across the eusps during valve closure. $A: p_t - p_1$; $B: \bar{p}_s - \bar{p}_A$.

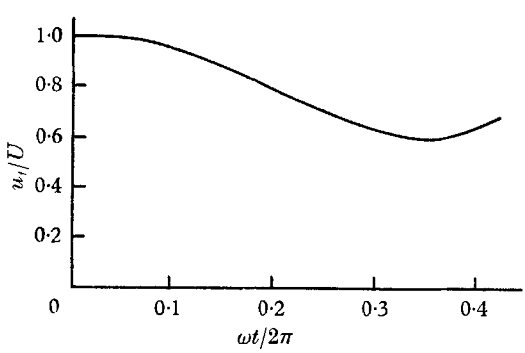

FIGURE 12. Cusp tip velocity.

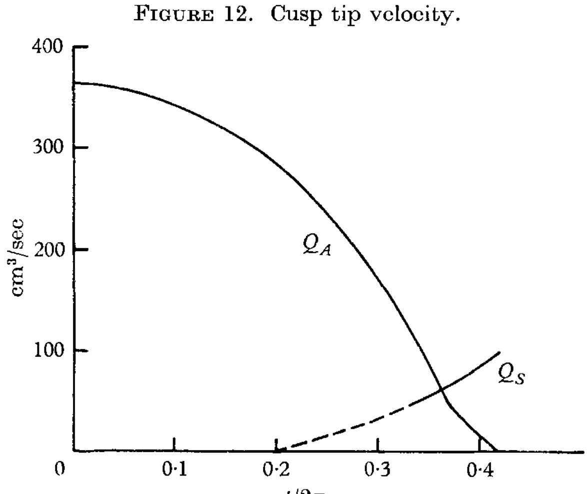

FIGURE 13. Volumetric flow in aorta, Q_A, and into sinus Q_S.

Unsteady vortex solution

The calculation above enabled us to find the average pressure on the aortic side of the cusps necessary to close the valve at the observed rate. This pressure has to be transmitted across the cusps, which are fixed to the aorta. We would expect

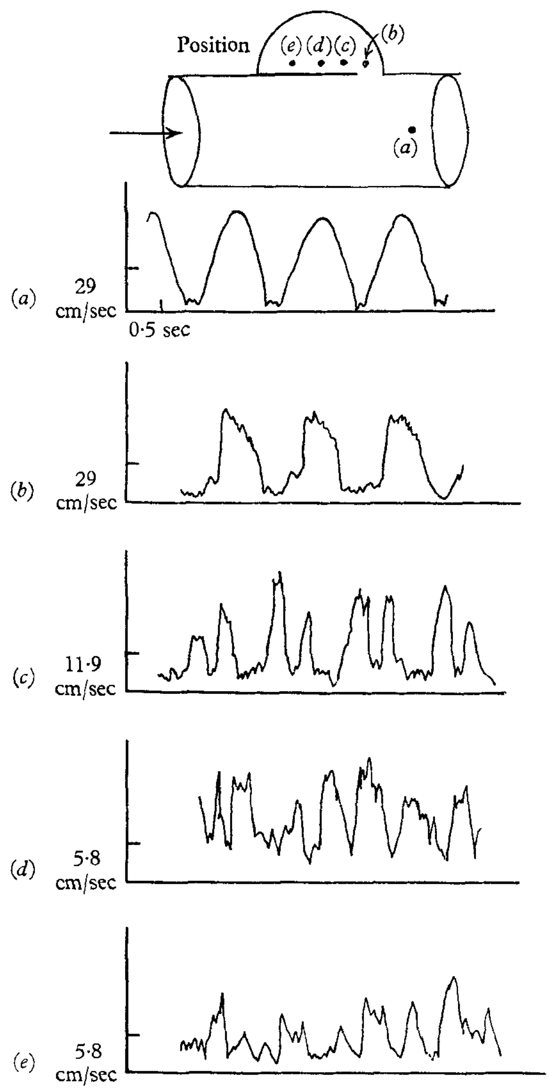

FIGURE 14. Velocity measurements in a sinus.

the pressure on the sinus-side of the cusps to exceed that on the aortic-side, and although differential pressure measurements in pulsatile flow were difficult to make, they were adequate to show that the pressure differences were of the order of one or two mm of mercury. In steady flow, differential pressure measurement is simple and accurate, and it was shown that sinus and free stream stagnation pressures were equal.

We seek to calculate the pressure difference across the cusps generated by the vortex mechanism in the early stages of closure, using the Hill vortex model developed above. The stream function given in (1) satisfies the full unsteady equations of axisymmetric motion if the parameter A (given by (12)) is constant, although the aortic velocity and pressure and the vortex radius may vary with time.

The assumption that A is constant is of doubtful value, since measurements of velocity in the sinuses indicate that the vortex velocity is tied to the aortic velocity in pulsatile flow. A better assumption would be a quasi-steady form of (12) and (16) with the steady velocity U replaced by the aortic velocity $u_1(t)$. In addition we require that the pressure at the sinus ridge, $p_0(t)$, is given by

$$p_0(t)-p_1(t) = \tfrac{1}{2}\rho u_1^2 - 2\rho a\,(du_1/dt), \tag{24}$$

which is an unsteady Bernoulli equation, and $p_1(t)$ is the pressure at the aortic ring (figure 10).

Assuming that the sinus and free-stream stagnation pressures are equal, as for the steady case, we obtain

$$\overline{p}_s(t)-p_1(t) = 0{\cdot}308\,(\tfrac{1}{2}\rho u_1^2) - 2\rho a\,(du_1/dt). \tag{25}$$

The pressure difference across the cusps, $\overline{p}_s - \overline{p}_A$, is plotted as a function of time in curve B of figure 11. This quasi-steady calculation is valid only for small values of $\omega t/2\pi$, but it does indicate that deceleration of the aortic flow will generate adequate pressure differences across the cusps during valve closure. Account has been taken of the slight divergence of the flow due to the projection of the cusps into the sinuses in their fully open position, which results in an increase in the pressure p_t just sufficient to make the pressure difference across the cusps vanish.

Evidence which lends support to the assumption that the vortex velocity is tied to the aortic velocity in pulsatile flow, is presented in figure 14. Measurements of velocity in the aorta and at four positions in the sinus show that the velocity within the sinus near the ridge, figure 14(*b*), where the vortex core is located in steady flow, is similar to the velocity in the aorta, figure 14(*a*), throughout the pulse. The velocity was measured with a heated element, which rectifies reversed flow. The relatively low peaks in velocity in the sinus at positions (*c*), (*d*) and (*e*) indicate that they are outside the main vortex region, but they do appear in pairs and lag the single peak obtained at position (*b*). This implies that the vortex core moves in an upstream direction (within the sinus) during valve closure, and that viscosity causes some reduction in vortex strength.

Conclusion

Experiments have shown that an essential feature of the operation of the aortic valve is the formation and maintenance of trapped vortices in the aortic sinuses, and this flow pattern has also been analyzed by means of a simple inviscid flow model. It appears that the vortical flow in the sinuses plays two distinct roles in the valve operation. During the period of maximum velocity in the aorta, when the valve is fully opened and the flow is quasi-steady, it acts as a control system which responds to valve cusp position, maintaining the valve cusps in a static fully opened configuration with the cusp tips protruding slightly into the sinus cavities. In the closure phase of the cycle, the trapped vortices persist because of their long decay time, and maintain a certain relationship between the time-varying sinus pressure and the sinus ridge stagnation pressure and contribute to the prevention of jet formation from the narrowing valve opening. The relationship between the sinus-ridge and sinus-cavity pressures is such that the unsteady-flow, axial, adverse pressure-gradient through the valve during flow deceleration provides the main force to close the valve and this force is effective in producing almost complete valve closure before a very small reversed-flow phase occurs.

This model of the fluid motion through the aortic valve leads to estimates for a lower bound to the Reynolds number and an upper bound to the Strouhal number for efficient valve operation, which appear to coincide with the limits found within the animal kingdom.

The authors wish to thank Mr F. H. Bellhouse and Dr K. G. Reid for their considerable assistance.

REFERENCES

Batchelor, G. K. 1956 *J. Fluid Mech.* **1**, 177.

Bellhouse, B. J. & Bellhouse, F. H. 1968 *Nature, Lond.* **217**, 86.

Bellhouse, B. J. & Reid, K. G. 1968 Submitted.

Burggraf, O. R. 1966 *J. Fluid Mech.* **24**, 113.

Leonardo da Vinci 1513 *Quaderni d'Anatomica* II, 9.

Milne-Thomson, L. M. 1960 *Theoretical Hydrodynamics*, 4th ed. New York: Macmillan.

Valsalva, A. M. 1740 *Opera Postuma*, Venice. (Latin.)

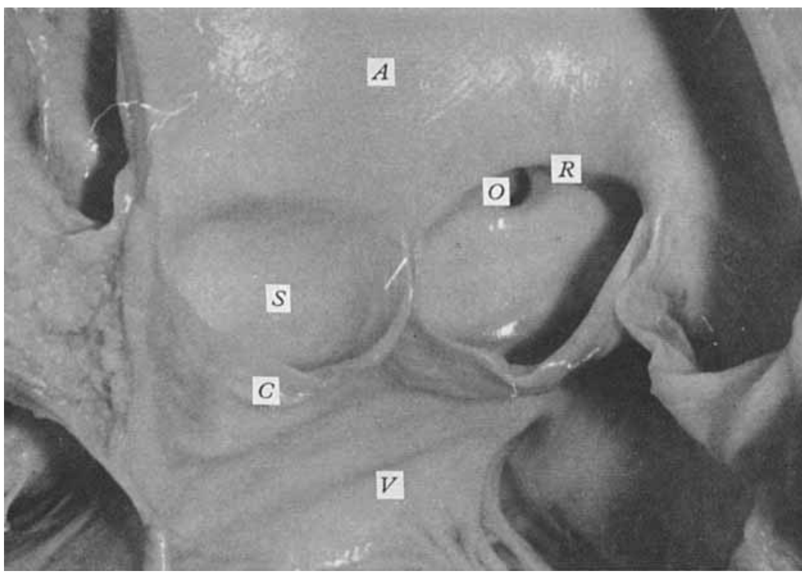

FIGURE 1. Photograph of human aortic valve, showing the cusps (C), sinuses (S) and one coronary ostium (O). Forward flow is from the left ventricle (V) to the aorta (A). Note the marked sinus ridges (R).

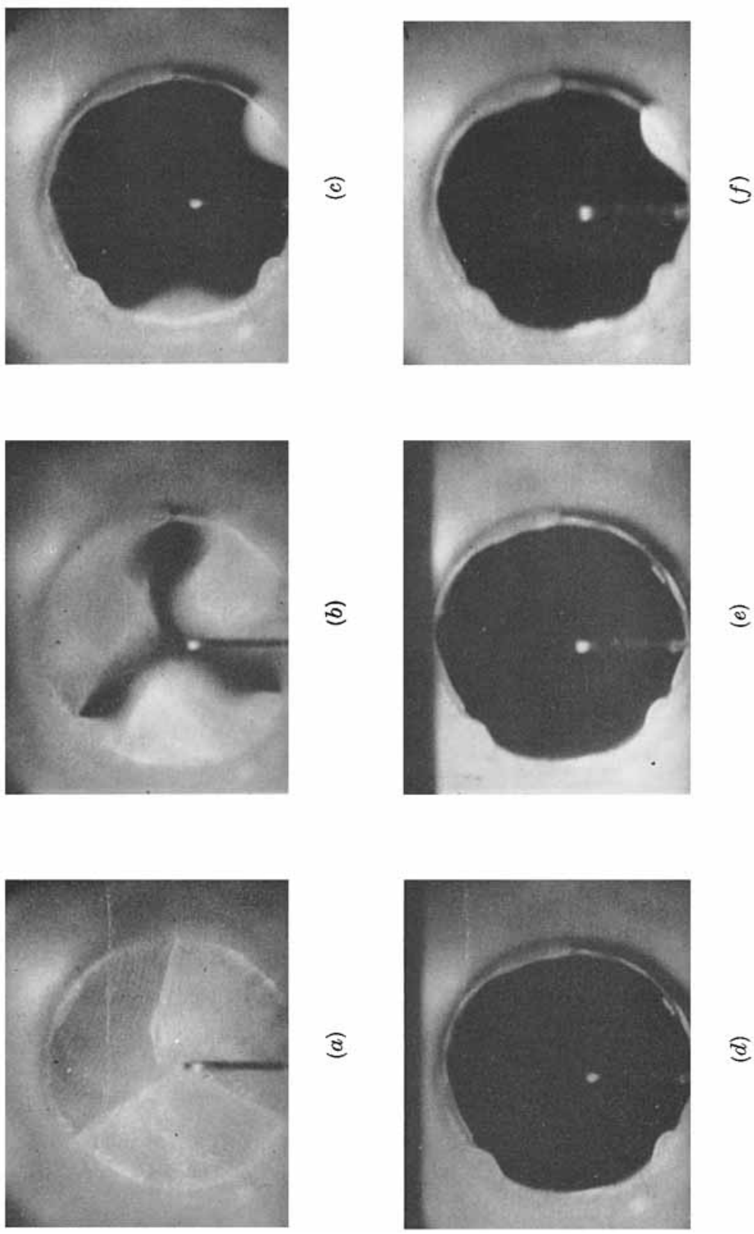

FIGURE 8. Photographs of successive frames of a ciné film of one cycle of the valve, viewed from the aorta with forward flow approaching the camera. Time interval between frames is 1/24th second.

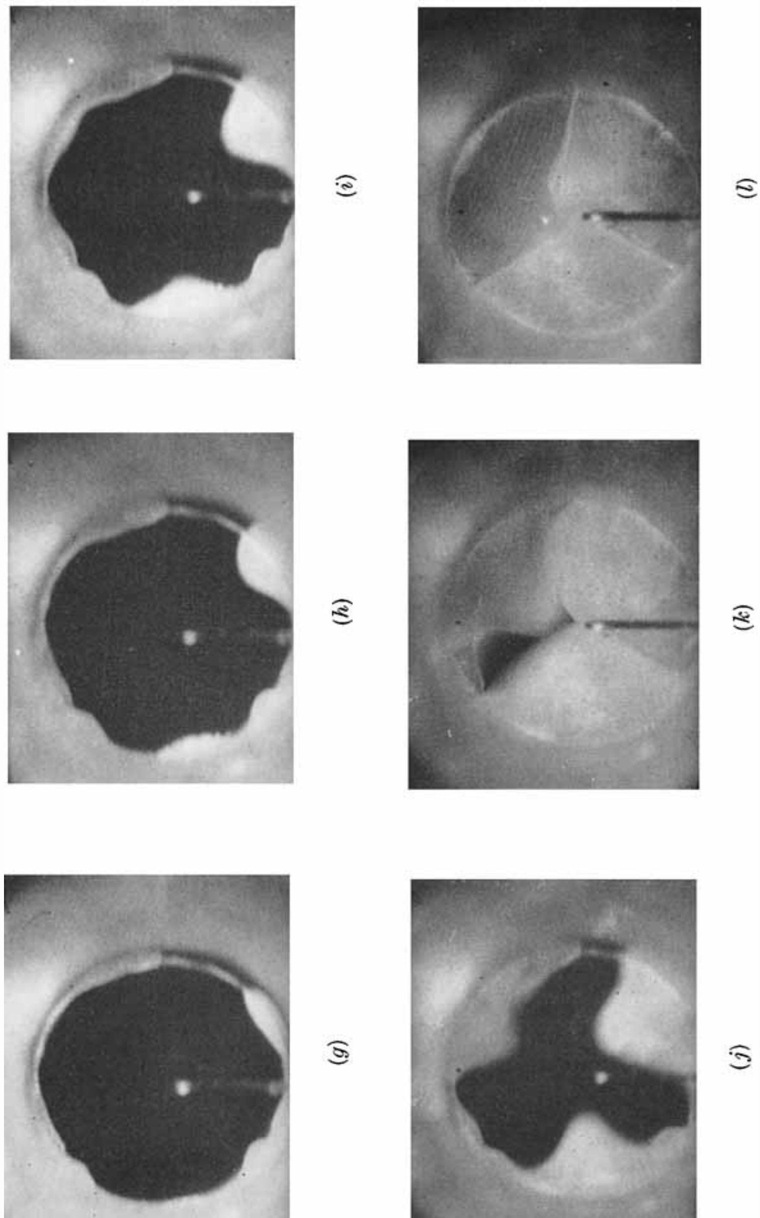

FIGURE 8. For legend see previous page.